Amplification of coherent synchrotron high harmonic emission from ultra-thin foils in relativistic light fields

J. Braenzel,[1,a)] A. A. Andreev,[1,2,b)] K. Y. Platonov,[3] L. Ehrentraut,[1] and M. Schnürer[1,c)]
[1]*Max Born Institute, Berlin 12489, Germany*
[2]*ELI-ALP, Szeged 6720, Hungary*
[3]*Peter the Great St. Petersburg Polytechnic University, St. Petersburg 195251, Russia*

(Received 19 April 2017; accepted 7 August 2017; published online 24 August 2017)

We report on a remarkable enhancement of high harmonic (HH) radiation emitted from the interaction of an ultra-intense laser pulse with ultra-thin foils by a manipulation of foil pre-plasma conditions. With a strong counter-propagating pre-pulse, we introduce a concerted expansion of the ultrathin foil target, and this significantly raises the efficiency of the HH generation process. Our experimental results show how the emission efficiency can be easily controlled by the intensity and delay time of the pre-pulse. The results give an important insight into the high harmonic generation process from solid dense plasmas when spatially limited. 1D particles in cell simulations confirm our experimental findings and show a significant dependency of the HH emission efficiency on the plasma density. The simplicity of the ultra-thin foil target and interaction geometry hold promise for specifically compact realization of imaging experiments with ultra-short and bright extreme ultra violet-pulses. *Published by AIP Publishing.* [http://dx.doi.org/10.1063/1.4999505]

High Harmonic (HH) radiation from intense laser pulse and dense plasma surface interactions is a promising source for brilliant coherent radiation with high photon energies and numbers. Compared to HH from gaseous media, the generation mechanism of relativistic HH from electron oscillations at solid-vacuum interfaces has no limitation in the driving laser's intensity. The high energetic cutoff of the emitted HH radiation scales with the relativistic gamma factor of the electrons' oscillations in the field at the illuminated plasma boundary.[1,2] The gamma factor, as the emitted photon number, is a function of the laser intensity.[2–4] The phenomenon of HH generation is equivalent to the emission of a coherent ultra-short light pulse once or twice per laser cycle with a single pulse duration smaller than the half laser period. This leads to the emission of an equally temporally spaced pulse train of ultrashort pulses. First, approaches to isolate a single as-pulse from the pulse train have been recently demonstrated.[5,6] For possible future applications, ultra-thin foil targets provide a simple setup that automatically and efficiently blocks the transmission of the fundamental frequency without major destruction of the temporal unique pulse characteristics.[7]

HH generation with solid state bulk targets at relativistic intensity is highly investigated.[8–10] There are different underlying generation mechanisms: the emission from a plasmon excitation, known as coherent wake emission (CWE),[11,12] the emission by the reflection from a relativistically oscillating (plasma) mirror (ROM),[2,4] and especially for foil targets a coherent synchrotron radiation emission (CSE).[1,3,7,13] Few publications investigated the HH generation by using ultrathin foil targets.[1,3,14–17] For HH radiation detected in the laser propagation direction behind the used target foil, the relativistic mirror model cannot be adapted without further modification.[3] The CWE model theoretically bases on the Brunel-absorption mechanism, leading to an electron bunch which excites plasma waves in its wake when penetrating through the plasma. These plasma waves can decay into coherent radiation that depends on the local density. Here, the maximum harmonic number is determined by the maximum target density $N_{max} = \omega_p/\omega$, with the plasma frequency $\omega_p = \sqrt{q^2 n_e/\varepsilon_0 m_e}$, where n_e is the electron density, q the elemental charge, ε_0 the dielectric constant for vacuum, ω the laser fundamental frequency, and m_e the electron mass. For nonrelativistic intensities up to the relativistic limit and oblique incidence angles, CWE emission from either target front side or inside the target or even a reemission from the target backside has been reported.[15,16,18] Nevertheless, for the laser at a normal incidence angle at the target, the Brunel absorption mechanism is not valid without further assumptions, e.g., denting of the target surface.[11,19] Hence, for the normal incidence geometry and relativistic intensities, the HH emission detected at the target rear side is usually explained by the CSE model. In this model, electron micro-bunches are formed at the plasma boundary, which experience high acceleration due to a rapid oscillatory motion and are accompanied by synchrotron-like emission of high frequency radiation. Due to this collective relativistic electron phenomenon, ultra-short high energetic and coherent light bursts are formed. Recent publications investigated the HH emission with respect to particular plasma boundary conditions and demonstrated that the efficiency of the ROM process[8,9,20] and the CSE process[1,7] is enhanced for a scale length of the plasma density gradient $L > 0.5\ \lambda_L$, while the CWE harmonic emission is suppressed for $L > 0.01\ \lambda_L$.[11,12,15]

In the following, we present that the HH-generation efficiency can be significantly raised when ultrathin

[a)]braenzel@mbi-berlin.de
[b)]andreev@mbi-berlin.de
[c)]schnuerer@mbi-berlin.de

foils are manipulated by a concerted pre-plasma expansion. Pre-heating the foil's backside with a strong laser pulse enlarges L and, for ultrathin foil, leads to overall expansion.[25] The reduction of the electron density has a significant influence on the laser plasma interaction and electron dynamics in the CSE process,[1] as it also determines the transmission characteristics. In general, radiation with a frequency $\omega > \omega_p$ can be transmitted through the plasma. Radiation with $\omega < \omega_p$ can penetrate the plasma in the order of the skin depth l_s, after which the field amplitude suffers from an exponential decay. For ultrathin foils with thicknesses $D \sim l_s$, a partial transmittance as function of the frequency results. We now show that by manipulation of the target density, a parametric optimum for the HH emission efficiency can be reached and controllably aligned.

Experiments were performed with the 70 TW Ti:Sapphire High Field Laser of the Max Born Institute. The laser system delivered a laser pulse duration of about 35 fs at ultrahigh laser contrast (10^{14}).[21] Figure 1 shows a schematic of the setup for the two counter-propagating laser pulse experiment. We used a beam splitter (75/25), and the resulting two pulses were focused on a freestanding plastic foil. The stronger laser pulse is named "drive pulse," while the transmitted, weaker part is referred to "P2 pulse." The intensity of the drive pulse I(D) = 6×10^{19} W/cm^2 was realized with a f/2 off axis parabolic mirror (OAP) (focal diameter, 4 μm; FWHM, 13% energy content). P2 passed a delay stage and was focused using a f/5.4 OAP (focal diameter, 30 μm; FWHM, 10% energy content) and reached an intensity up to $I_P = 10^{18}$ W/cm^2. The experiment allowed a spatial overlap of both laser pulses on the target of about ± 10 μm. The temporal overlap between both laser pulses was determined within an uncertainty of ± 0.3 ps by a plasma spark shadowgraph measurement. This uncertainty introduces a possible constant offset of the temporal overlap within the same experimental run. We detected the emitted extreme ultra violet (XUV) radiation in the direction of the drive pulse using a gold transmission grating with 1940 lines/mm. The diffracted XUV-light was detected with a Hamamatsu MCP, 100 mm in diameter. For targets, we used plastic foils [poly-vinyl-formal PVF, $C_5H_7O_2$; density, 1.23 g/cm^3 (Ref. 22)] in the thickness range of 12–85 nm. The electron density of the fully ionized ultrathin foil is about $n_e = 220 n_c$, where $n_c = \varepsilon_0 \omega^2 / q^2$. In various measurements, with solely using the drive pulse, high fluctuations in the HH intensity of up to 50% were observed. Qualitatively comparable spectra were obtained from different foil thicknesses. The maximum harmonic order ranged between 15 and 17, and harmonic lines in a higher energy range could not be distinguished without ambiguities from the incoherent XUV background. An example can be found in Figs. 2 and 3 for two different foil thicknesses (35 and 85 nm). The displayed spectra are not calibrated. Note that the detector's efficiency has a nonlinear response dependent on the photon energy and could be less sensitive than one order of magnitude for the spectral range of >100 nm.[23]

When the target foil was preheated by the P2 pulse with an intensity of about $0.3 - 1 \times 10^{18}$ W/cm^2 few ps before the drive pulse arrived, we detected a significant and reproducible enhancement in the HH intensity up to one order of magnitude. This amplified HH emission sets in for a particular delay time and applied pre-pulse intensity. Figure 2 shows a direct comparison between a reference measurement without and one with using the pre-pulse at the optimum delay time. We excluded experimentally any HH emission driven by the pre-pulse in the backward direction by applying the P2 pulse with circular field polarization[6] or by a direct measurement without the drive pulse. CWE emission could set in for $I > 10^{16}$ W/cm^2, and hence, the P2 pulse could have been strong enough to drive CWE emission itself. Since this was not the case here, this gives a strong indication that the CWE process is inhibited or highly suppressed for normal incidence geometry. It can be seen in Fig. 2 that for a spectral range above >100 nm, half integer harmonics for either the unheated or heated case were detected, which indicates a plasmonic involvement up to a certain frequency. However, the CWE-like process as discussed in Ref. 16 is clearly connected to the plasma frequency and should display a changed emission cutoff for an expanded foil, as in addition, should be suppressed for an enlarged density ramp.[12] As shown in Fig. 2 and for even longer delay times in Fig. 3, N_{max} of the expanded foil is equal or even higher

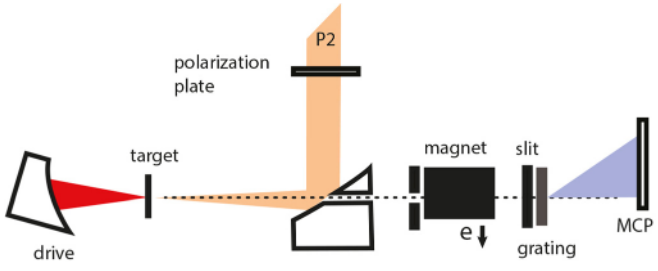

FIG. 1. Setup for the two laser pulse experiment in a counter-propagating geometry. The second, less intense laser pulse (orange) hits the target's backside at normal incidence. XUV radiation was detected in the propagation direction of the stronger, drive (red) laser pulse.

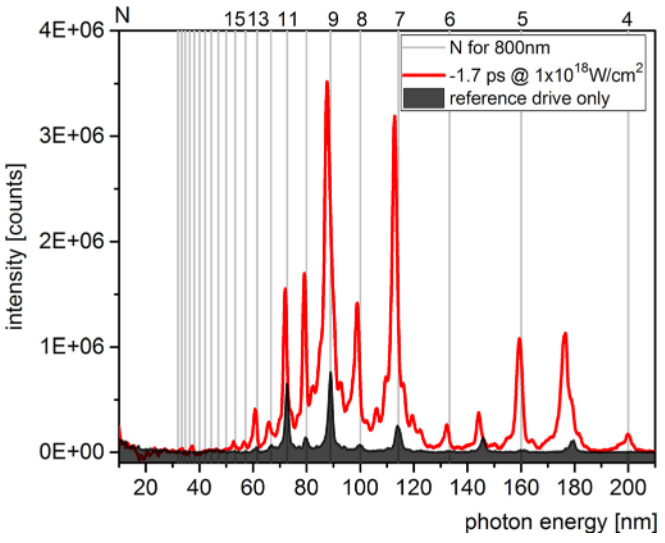

FIG. 2. High harmonic radiation detected from the interaction between the drive laser pulse (reference) with a 35 nm PVF foil and with pre-heating the target with the P2 pulse at a delay of −1.7 ps. The spectrum was background corrected concerning incoherent XUV radiation. The polarization for both laser pulses was linear and perpendicular to each other.

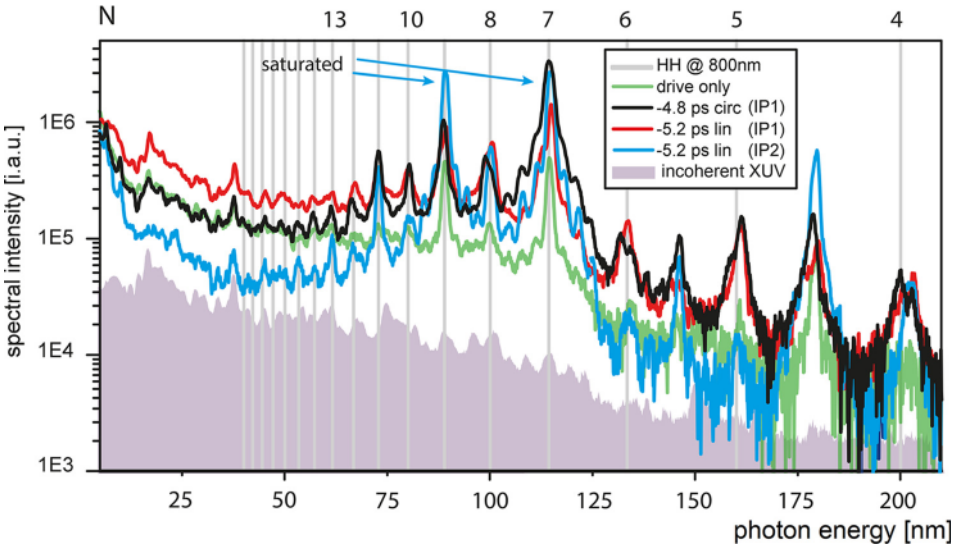

FIG. 3. Amplification for the pre-manipulated plasma condition and dependency on delay and intensity of the P2 pulse. $I_{P1} = 1 \times 10^{18}$ W/cm^2, $I_{P2} = 3 \times 10^{17}$ W/cm^2 at different polarizations and an 85 nm PVF foil. The measured incoherent plasma spectrum is plotted with a scaled intensity in light purple in order to illustrate its typical spectral distribution. The corresponding signal to noise values are 2:1 (green), 3:1 (black), 0.8:1 (red), and 6:1 (blue).

than the one obtained from the unheated foil. In the following, our numerical simulation and discussion are therefore based on the CSE model which was recently studied in detail in Refs. 1 and 7.

Pre-heating significantly stabilized the HH emission compared to the fluctuations in the reference signal. Preheating of ultrathin foils leads to an expansion of the plasma boundary with at least the sound speed of the ions of about 10^6 m/s. Hence, such an expansion can decrease the electron density of a fully ionized ultrathin foil by a factor of almost one order of magnitude in a few ps. Since the intensity of our pre-pulse reaches the onset of the Target Normal Sheath Acceleration (TNSA) acceleration, the temporal and spatial density evolution of the foil has to be considered highly complex.

For the same laser intensities (drive and P2), the measured HH intensity changed with the delay time applied. Table I gives the relative HH intensity enhancement for different delay times with respect to the reference measurement. The detected spectra, as can be seen in Fig. 3, always consist of coherent and incoherent XUV contents. In order to show that the laser energy transforms for a particular pre-plasma condition into coherent rather than into incoherent radiation, a comparison of the contrast ratio of the HH spectrum is given in Table I. For approximating the incoherent content for the spectral distribution between 10–240 nm, we used a measurement at lower laser contrast (cf. Fig. 3) and linearly aligned it to each HH-measurement such that in all HH-spectra, the plasma line at 16.9 nm exhibited the same intensity. Table I gives the evaluated signal to noise ratios (SNR) between this incoherent and the coherent spectral content for various delay times of the P2 pulse. The contrast ratio is smaller or equal to the reference measurements for various delay times, except for the optimum range. The high SNR values in our optimum parametric range reveal a higher conversion efficiency from the laser into coherent HH emission. From this, we follow that simply an enhanced transmission through the foil cannot explain the increase in the HH intensity in the optimum parametric range. These results confirm the theoretical work in Ref. 1 where an optimum density and density profile for the CSE harmonic emission are predicted.

TABLE I. Relative amplification and the signal to noise ratio of the integrated HH signal.

Delay[a]	$I_{HH}/I_{ref.}$[b]	SNR[c]
Reference	1	5:1
−0.7 ps	1.3	3:1
−1.0 ps	2.0	3:1
−1.3 ps	2.7	4:1
−1.7 ps	13.0	8:1
−3.3 ps	3.0	4:1

[a]Gives the delay time of the second laser pulse.
[b]Integrated HH signal relative to the reference measurement, both for the spectral range of 30–140 nm and without the incoherent XUV content.
[c]Signal to noise ratio (SNR) gives the ratio between the coherent and the incoherent content for the corresponding measurement and the same spectral range.

We approximated the energy content of the high harmonic radiation by using a cross-calibration between the used MCP-detector and an absolutely calibrated XUV-CCD at the Al-Ledge. We extrapolated this calibration to the harmonic line N = 9 by assuming an emission cone of 0.4° (Ref. 24) and a flat MCP-response between 17 and 90 nm. Thereby, we estimated an energy content of about 10^{-7} J for N = 9. Since the detector efficiency drops down for the low energetic energy range, this number can give a first impression.

The optimized regime is determined by the interplay between delay time and the intensity of the pre-pulse. This is shown in Fig. 3, where the highest HH emission was measured at different delay times when different pre-pulse intensities were applied. The optimum regime is found at much longer delay times, when the polarization of the pre-pulse was changed to circular, since this probably decreases the laser field amplitude by $0.5^{-1/2}$. As a proof of principle, we applied the P2 pulse with a lower intensity (IP2) at linear polarization and detected the optimum range at longer delay times. These findings suggest a simple way to obtain a favorable density preparation of the target by making use of the

expansion velocity as a function of the applied heating intensity.

In order to test theoretically the influence of the HH emission for an expanded target, we performed numerical analysis in one dimension using the modified Lichter's Particle in Cell (LPIC) code.[2] With using comparable parameters of the experimental setup from above, in the simulation the laser interacted with a fully ionized carbon plasma. We applied to different densities and thicknesses, both with a rectangular density shape. Hence, in the first approach, we investigated the impact of the target density, in contrast to the scale length variation of the plasma density gradient in Refs. 9, 12, and 20. In the simulation, the unheated plasma was considered with an initial foil thickness of 35 nm and ion densities of $n_i = 33n_c$ and $n_e = 198n_c$ and the expanded target with $n_e = 66n_c$ and a thickness of 105 nm. The emitted radiation from the single laser pulse interaction in the forward direction of the laser pulse is shown in Fig. 4. This HH radiation has passed the target foil, and similar to the experimental results of former publications,[3,14,18] the intensity of the lower harmonic numbers is partly suppressed by the opacity of the plasma.

In the case of the expanded plasma, the simulation delivered a significant increase in the HH radiation. Next to the higher HH-intensity, the characteristics of intensity decay with the harmonic number N changed. With our present understanding, the foil expansions and thus density reduction have a two-fold effect which needs to be further analyzed in detail: The intense light field couples and interacts with more electrons coherently as suggested in Refs. 1 and 7, and thus, the HH emission is enhanced. Moreover, the foil expansion allows complete electron excursions through the foil to be driven in resonance with the light cycle. This transfers higher energy into the electron ensemble, which also enhances the HH emission. A simulation test with different density profiles showed no differences in emission scaling; eventually, differences at low order HH emission are indicated. As a future aim, an analytical approach will be developed in order to obtain a parametric dependency between the plasma density and the collective oscillatory electron motion with subsequent emission of EM radiation.

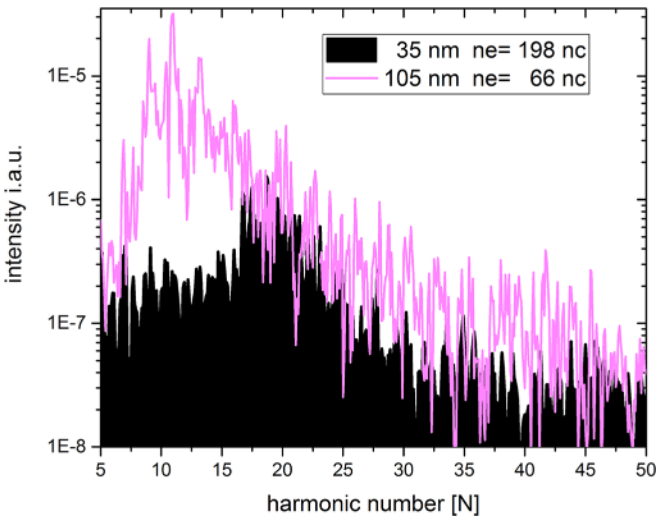

FIG. 4. Coherent radiation behind the illuminated foil out of the 1D LPIC simulation for two different foil thicknesses and densities, according to a pre-expanded target foil.

In conclusion, we demonstrated a significantly enhanced HH emission from laser driven ultra-thin foils for a manipulated pre-plasma condition. Due to a high intensity and ultrashort duration of our counter-propagating heating laser, next to an expansion of the foil boundary, a decrease in the foil's density has to be considered. We have shown experimentally that by this method, the HH intensity at the foil rear side can be increased more than one order of magnitude. The simulation results confirmed a significant enhancement of the HH intensity at the foil's back side that can partially be attributed to a higher transmission of the radiation through the plasma and to the optimal density range for the electron bunch kinematics according the CSE model. Our results confirm an optimal parametric plasma regime for CSE emission as predicted in Refs. 1 and 7 that can be easily prepared by the intensity and delay time of the second laser pulse. This preplasma condition needs a detailed study in upcoming experimental and theoretical work. The experiments showed, to our knowledge, for the first time, that it is possible to manipulate the laser plasma interaction by such strong pre-pulses and that this enables an overall density manipulation. This promises a novel perspective to align important parameters for the relativistic laser plasma interaction. Moreover, the applied interaction and HH-generation setup is very compact and also cost-effective, thus providing new possibilities for imaging or probing experiments with bright, ultra-fast and single shot XUV-pulses.

The research leading to these results received funding from the Deutsche Forschungsgemeinschaft within the Program CRC/Transregio 18 and LASERLAB-EUROPE (Grant No. 284464, EC's Seventh Framework Program). Computational resources were provided by the JSC within the Project No. HBU15 and by the John von Neumann Institute for Computing (NIC), providing us access on JUROPA at the Jülich Supercomputing Centre (JSC). Furthermore, we thank D. Sommer (MBI) for his excellent work on the target foil production.

[1]M. Cherednychek and A. Pukhov, Phys. Plasmas **23**(10), 103301 (2016).
[2]R. Lichters, J. Meyer-ter-Vehn, and A. Pukhov, Phys. Plasmas **3**(9), 3425 (1996).
[3]B. Dromey, S. Rykovanov, M. Yeung, R. Horlein, D. Jung, D. C. Gautier, T. Dzelzainis, D. Kiefer, S. Palaniyppan, R. Shah, J. Schreiber, H. Ruhl, J. C. Fernandez, C. L. S. Lewis, M. Zepf, and B. M. Hegelich, Nat. Phys. **8**(11), 804 (2012).
[4]S. V. Bulanov, T. Zh Esirkepov, M. Kando, and J. Koga, Plasma Sources Sci. Technol. **25**(5), 053001 (2016).
[5]J. A. Wheeler, A. Borot, S. Monchoce, H. Vincenti, A. Ricci, A. Malvache, R. Lopez-Martens, and F. Quere, Nat. Photonics **6**(12), 829 (2012); H. Vincenti and F. Quéré, Phys. Rev. Lett. **108**(11), 113904 (2012).
[6]M. Yeung, B. Dromey, S. Cousens, T. Dzelzainis, D. Kiefer, J. Schreiber, J. H. Bin, W. Ma, C. Kreuzer, J. Meyer-ter-Vehn, M. J. V. Streeter, P. S. Foster, S. Rykovanov, and M. Zepf, Phys. Rev. Lett. **112**(12), 123902 (2014).
[7]S. Cousens, B. Reville, B. Dromey, and M. Zepf, Phys. Rev. Lett. **116**(8), 083901 (2016).

[8]M. Yeung, S. Rykovanov, J. Bierbach, L. Li, E. Eckner, S. Kuschel, A. Woldegeorgis, C. Rödel, A. Sävert, G. G. Paulus, M. Coughlan, B. Dromey, and M. Zepf, Nat. Photonics **11**(1), 32 (2017).
[9]C. Rödel, D. an der Brügge, J. Bierbach, M. Yeung, T. Hahn, B. Dromey, S. Herzer, S. Fuchs, A. Galestian Pour, E. Eckner, M. Behmke, M. Cerchez, O. Jäckel, D. Hemmers, T. Toncian, M. C. Kaluza, A. Belyanin, G. Pretzler, O. Willi, A. Pukhov, M. Zepf, and G. G. Paulus, Phys. Rev. Lett. **109**(12), 125002 (2012).
[10]J. Braenzel, A. Andreev, M. Schnürer, S. Steinke, K. Platonov, G. Priebe, and W. Sandner, Phys. Plasmas **20**(8), 083109 (2013); M. Behmke, D. an der Brügge, C. Rödel, M. Cerchez, D. Hemmers, M. Heyer, O. Jäckel, M. Kübel, G. G. Paulus, G. Pretzler, A. Pukhov, M. Toncian, T. Toncian, and O. Willi, Phys. Rev. Lett. **106**(18), 185002 (2011); B. Dromey, M. Zepf, A. Gopal, K. Lancaster, M. S. Wei, K. Krushelnick, M. Tatarakis, N. Vakakis, S. Moustaizis, R. Kodama, M. Tampo, C. Stoeckl, R. Clarke, H. Habara, D. Neely, S. Karsch, and P. Norreys, Nat. Phys. **2**(7), 456 (2006); S. Monchocé, S. Kahaly, A. Leblanc, L. Videau, P. Combis, F. Réau, D. Garzella, P. D. Oliveira, P. Martin, and F. Quéré, Phys. Rev. Lett. **112**(14), 145008 (2014).
[11]F. Quéré, C. Thaury, P. Monot, S. Dobosz, Ph. Martin, J. P. Geindre, and P. Audebert, Phys. Rev. Lett. **96**(12), 125004 (2006); C. Thaury and F. Quéré, J. Phys. B: At., Mol. Opt. Phys. **43**(21), 213001 (2010).
[12]M. Bocoum, M. Thévenet, F. Böhle, B. Beaurepaire, A. Vernier, A. Jullien, J. Faure, and R. Lopez-Martens, Phys. Rev. Lett. **116**(18), 185001 (2016).
[13]D. der Brugge and A. Pukhov, Phys. Plasmas **17**(3), 033110 (2010).
[14]D. Kiefer, M. Yeung, T. Dzelzainis, P. S. Foster, S. G. Rykovanov, C. Ls Lewis, R. S. Marjoribanks, H. Ruhl, D. Habs, J. Schreiber, M. Zepf, and B. Dromey, Nat. Commun. **4**, 1763 (2013); K. Krushelnick, W. Rozmus, U. Wagner, F. N. Beg, S. G. Bochkarev, E. L. Clark, A. E. Dangor, R. G. Evans, A. Gopal, H. Habara, S. P. D. Mangles, P. A. Norreys, A. P. L. Robinson, M. Tatarakis, M. S. Wei, and M. Zepf, Phys. Rev. Lett. **100**(12), 125005 (2008).
[15]B. Dromey, S. G. Rykovanov, D. Adams, R. Horlein, Y. Nomura, D. C. Carroll, P. S. Foster, S. Kar, K. Markey, P. McKenna, D. Neely, M. Geissler, G. D. Tsakiris, and M. Zepf, Phys. Rev. Lett. **102**(22), 225002 (2009).
[16]U. Teubner, K. Eidmann, U. Wagner, U. Andiel, F. Pisani, G. D. Tsakiris, K. Witte, J. Meyer-ter-Vehn, T. Schlegel, and E. Förster, Phys. Rev. Lett. **92**(18), 185001 (2004); K. Eidmann, T. Kawachi, A. Marcinkevičius, R. Bartlome, G. D. Tsakiris, K. Witte, and U. Teubner, Phys. Rev. E **72**(3), 036413 (2005).
[17]V. A. Vshivkov, N. M. Naumova, F. Pegoraro, and S. V. Bulanov, Phys. Plasmas **5**(7), 2727 (1998).
[18]H. George, F. Quere, C. Thaury, G. Bonnaud, and P. Martin, New J. Phys. **11**, 113028 (2009).
[19]F. Brunel, Phys. Rev. Lett. **59**(1), 52 (1987). R. Hörlein, S. Steinke, A. Henig, S. G. Rykovanov, M. Schnürer, T. Sokollik, D. Kiefer, D. Jung, X. Q. Yan, T. Tajima, J. Schreiber, M. Hegelich, P. V. Nickles, M. Zepf, G. D. Tsakiris, W. Sandner, and D. Habs, Laser Part. Beams **29**(4), 383 (2011).
[20]S. Kahaly, S. Monchocè, H. Vincenti, T. Dzelzainis, B. Dromey, M. Zepf, Ph. Martin, and F. Quèrè, Phys. Rev. Lett. **110**(17), 175001 (2013).
[21]M. Kalashnikov, K. Osvay, R. Volkov, H. Schönnagel, and W. Sandner, paper presented at the CLEO:2011 - Laser Applications to Photonic Applications, Baltimore, Maryland, 2011.
[22]J. Braenzel, C. Pratsch, P. Hilz, C. Kreuzer, M. Schnurer, H. Stiel, and W. Sandner, Rev. Sci. Instrum. **84**(5), 056109 (2013).
[23]Hamamatsu, http://www.hamamatsu.com/jp/en/3008.html for Manual MCP assembly (2017).
[24]Our approximation did not take the efficiency of the MCP detector into account. The emission cone scales with the harmonic number 24. So far.
[25]M. Gauthier, S. N. Chen, A. Levy, P. Audebert, C. Blancard, T. Ceccotti, M. Cerchez, D. Doria, V. Floquet, E. Lamour, C. Peth, L. Romagnani, J.-P. Rozet, M. Scheinder, R. Shepherd, T. Toncian, D. Vernhet, O. Willi, M. Borghesi, G. Faussurier, and J. Fuchs, Phys. Rev. Lett. **110**, 135003 (2013).